THE JOURNAL OF BIOLOGICAL CHEMISTRY VOL. 286, NO. 9, pp. 6879–6889, March 4, 2011

Two Serine Residues Control Sequential Steps during Catalysis of the Yeast Copper ATPase through Different Mechanisms That Involve Kinase-mediated Phosphorylations*

Received for publication, December 1, 2010 Published, JBC Papers in Press, December 16, 2010, DOI 10.1074/jbc.M110.207704

Rafael H. F. Valverde[‡§1], Thiago Britto-Borges[‡§], Jennifer Lowe[‡§], Marcelo Einicker-Lamas[‡§], Elisabeth Mintz[¶‖], Martine Cuillel[¶‖**2], and Adalberto Vieyra[‡§3]**

*From the [‡]Instituto de Biofísica Carlos Chagas Filho and the [§]Instituto Nacional de Ciência e Tecnologia em Biologia Estrutural e Bioimagem, Universidade Federal do Rio de Janeiro, 21949-900 Rio de Janeiro, Brazil and [¶]CEA, DSV, iRTSV, Laboratoire de Chimie et Biologie des Métaux, 17 Rue des Martyrs, Grenoble F-38054, the [‖]CNRS UMR 5249, Grenoble F-38054, and the **Université Joseph Fourier, Grenoble F-38000, France*

Ccc2, the yeast copper-transporting ATPase, pumps copper from the cytosol to the Golgi lumen. During its catalytic cycle, Ccc2 undergoes auto-phosphorylation on Asp^{627} and uses the energy gained to transport copper across the cell membrane. We previously demonstrated that cAMP-dependent protein kinase (PKA) controls the energy interconversion $^{Cu}E\sim P \rightarrow E\text{-}P + Cu$ when Ser^{258} is phosphorylated. We now demonstrate that Ser^{258} is essential *in vivo* for copper homeostasis in extremely low copper and iron concentrations. The S258A mutation abrogates all PKA-mediated phosphorylations of Ccc2, whereas the S971A mutation leads to a 100% increase in its global regulatory phosphorylation. With S258A, the first-order rate constant of catalytic phosphorylation by ATP decreases from 0.057 to 0.030 s^{-1}, with an 8-fold decrease in the burst of initial phosphorylation. With the S971A mutant, the rate constant decreases to 0.007 s^{-1}. $PKAi_{5-24}$ decreases the amount of the aspartylphosphate intermediate (EP) in Ccc2 wt by 50% within 1 min, but not in S258A, S971A, or S258A/S971A. The increase of the initial burst and the extremely slow phosphorylation when the "phosphomimetic" mutant S258D was assayed ($k = 0.0036\ s^{-1}$), indicate that electrostatic and conformational (non-electrostatic) mechanisms are involved in the regulatory role of Ser^{258}. Accumulation of an ADP-insensitive form in S971A demonstrates that Ser^{971} is required to accelerate the hydrolysis of the E-P form during turnover. We propose that Ser^{258} and Ser^{971} are under long-range intramolecular, reciprocal and concerted control, in a sequential process that is crucial for catalysis and copper transport in the yeast copper ATPase.

Copper plays an essential role in all known organisms. Transition metal properties give it the capacity to accept and donate electrons, and therefore to act as a cofactor in a broad diversity of enzymes that catalyze a great variety of reactions (1). Different active copper transporters (Cu(I)-ATPases) present in prokaryotes and eukaryotes (1–4) play a pivotal role in the homeostatic control of intracellular metal concentration. Active copper transport in mammals is mediated by two different ATPases: ATP7A (the Menkes ATPase) and ATP7B (the Wilson ATPase). Whereas ATP7A is ubiquitous, ATP7B is predominantly expressed in hepatocytes and in distinct scattered cell types in the central nervous system, kidney, placenta, and mammary glands (5). In humans, impaired copper delivery to the secretory/biosynthetic pathway and the circulatory system leads to severe conditions such as Wilson and Menkes diseases.

Just as mammalian cells have machinery for copper homeostasis, *Saccharomyces cerevisiae* contains homologous proteins for each corresponding function, physiologically coupling copper capture, intracellular trafficking, and delivery to a variety of acceptors. The yeast Cu(I)-ATPase, known as Ccc2, transports copper to protein acceptors in the lumen of the Golgi complex (6). Copper delivery to the *trans* Golgi network (TGN)[4] lumen is essential for iron metabolism in yeast, as the iron transporter Ftr1p must be activated by Fet3p in the TGN, which requires copper as a cofactor (7). Therefore, the role of Ccc2 in iron metabolism in yeast is similar to that in mammalian ATP7B with respect to ceruloplasmin, a protein synthesized in the hepatocyte TGN (8). For this reason, *S. cerevisiae* is a valuable model for studying copper homeostasis.

Considerable progress has been made toward elucidating catalytic phosphorylation by Cu(I)-ATPases (4, 9, 10); these are members of the ATPase family harboring the highly conserved DKTGT motif (11) (Fig. 1*A*). However, few reports have addressed the role of their kinase-mediated regulatory phosphorylation in the subcellular traffick-

* This work was supported by ÉGIDE (France), CAPES/COFECUB (Brazil/France) and the CAPES National Program of Post-doctoral Training (Brazil), the Rio de Janeiro State Funding Agency (FAPERJ, Brazil), the Brazilian Research Council (CNPq, Brazil), and the Programme de Toxicologie Nucléaire Environnementale (France).

This work is dedicated to Darcy Fontoura de Almeida on his 80th birthday.

[1] Recipient of a fellowship from the CAPES/PNPD Program.

[2] To whom correspondence may be addressed. Tel.: 33-4-38789651; Fax: 33-4-38785487; E-mail: martine.cuillel@cea.fr.

[3] To whom correspondence may be addressed. Tel.: 55-21-25626521; Fax: 55-21-22808193; E-mail: avieyra@biof.ufrj.br.

[4] The abbreviations used are: TGN, *trans* Golgi network; E∼P, high-energy phosphoenzyme; E-P, low-energy phosphoenzyme; $PKAi_{5-24}$, PKA inhibitor peptide 5–24; pkaPS, PKA prediction sites.

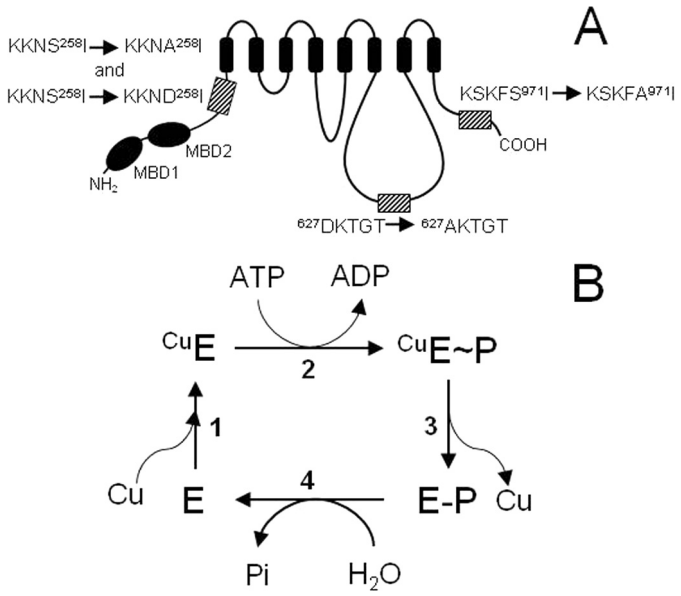

FIGURE 1. **Schematic representation of Ccc2 and its mutants, and proposed catalytic cycle of ATP hydrolysis and copper translocation.** *A*, S258A, S258D, S971A, S258A/S971A, and D627A mutants were created by site-directed mutagenesis as described under "Experimental Procedures." In S258A, S971A, and D627A, Ala replaces Ser^{258}, Ser^{971}, and Asp^{627}, respectively, as highlighted by the *hatched boxes* in the representation of the Ccc2 topological structure. In S258D, Asp replaces Ser^{258}. The *small arrows* between the sequences indicate the mutations and MDB1 and MDB2 represent the two metal-binding domains in the N-terminal region of Ccc2. For the sake of simplicity, the double-mutant S258A/S971A has been omitted. *B*, catalytic cycle proposed for Ccc2. Copper binding to the pump (*step 1*), phosphorylation by ATP (*step 2*), conversion of the high-energy E~P form to the low-energy E-P form and copper release (*step 3*) and hydrolysis of the phosphorylated intermediate (*step 4*) are the main steps in the reaction that actively transports copper from the cytosol to acceptor proteins in the Golgi lumen (10).

ing and localization of the copper pumps, particularly in response to copper levels (12–14). The involvement of a cyclic AMP-dependent kinase (PKA) in the intracellular movement of ATP7A in response to increased intracellular copper concentration was demonstrated by Cobbold *et al.* (13), and more recent studies point to the occurrence of kinase-mediated phosphorylation in different domains of both the human Cu(I)-ATPases (14, 15). The importance of regulatory phosphorylation for the catalytic cycle was recently demonstrated for ATP7B (16).

Our group has demonstrated that Ser^{258} of Ccc2 is the target for copper-dependent PKA-mediated phosphorylation, which is crucial for correct energy interconversion at the E~P → E-P step of the catalytic cycle (17). The physiological relevance of PKA-mediated phosphorylation of this serine is evident; its mutation to Ala leads to the progressive accumulation of the ^{Cu}E~P form as long as Ccc2 undergoes turnover. This serine residue, which has the highest score for PKA phosphorylation in Ccc2 (17), is located at the boundary between the N-terminal domain and the ATPase core. Because the N-terminal domain acts as a copper sensor for catalysis in Cu(I)-ATPases (15, 16, 18), we investigated whether copper-dependent PKA-mediated phosphorylation of Ser^{258} modulates the early steps of the catalytic cycle that involve copper handling: the transition Cu(I) + E → ^{Cu}E and the subsequent phosphoryl transfer ATP + ^{Cu}E → ^{Cu}E~P + ADP (Fig. 1*B*) (10), where Asp^{627} in the active site is the acceptor of the γ-phosphoryl group. In addition, we investigated the possible regulatory role of another serine residue with a high score for PKA recognition and phosphorylation, *i.e.* Ser^{971} (17), which is located at the end of Ccc2 C terminus.

EXPERIMENTAL PROCEDURES

Materials—ATP (sodium salt), the copper chelators BCA and BCS, protein kinase A inhibitor peptide 5–24 (PKAi$_{5-24}$) and protein A-agarose were purchased from Sigma. The anti-PKA polyclonal antibody was obtained from Calbiochem. [γ-^{32}P]ATP was purchased from Perkin Elmer or prepared from ^{32}P$_i$ (IPEN) as described by Maia *et al.* (19). The anti-Ccc2 polyclonal rabbit antibody used for immunoprecipitation and immunodetection was that previously described (10). The kit PlusOne™ (Amersham Biosciences) was used for protein silver staining in gels.

Yeast Strains—The ΔCCC2 yeast strain and yeast transformants (Ccc2 wt, D627A and S258A) were obtained as previously described (10). Each mutant was used and subcloned in the single copy plasmid. This plasmid, which contains the HIS3 selection factor and the PMA1 promoter, was used for expression in *S. cerevisiae*. The mutants were subcloned in the pFastBac1 plasmid for expression using the baculovirus/*Sf*9 system (Invitrogen).

In Vivo Assays—Transformed yeast strains were selected on Drop Out without selection factor. Growth curves of yeast cells expressing Ccc2 (wt, D627A or S258A variants), were studied using two different media. They were grown on a yeast nitrogen base (YNB, without Cu and Fe) supplemented with amino acids, except for leucine and histidine, and 1 μM $CuSO_4$, 50 μM $NH_4(FeSO_4)_2{\cdot}6H_2O$, and 1 mM ferrozine at 30 °C (20). This medium is described as iron-limited and was used to demonstrate the importance of Ser^{258} for cell growth and survival. A copper-supplemented medium (500 μM $CuSO_4$) was also employed. To obtain the growth curves of yeast strains, saturated yeast cultures grown in DOB medium were sedimented and resuspended in fresh iron-limited medium or copper-supplemented medium. This pre-culture was used to inoculate cultures at a density of A_{600} = 0.1. Cultures were grown at 30 °C for 38 h and monitored spectroscopically at the times indicated in Fig. 2.

Wild-type and Mutated CCC2 Gene—Isolation of genomic DNA from *S. cerevisiae* (strain 288c) and amplification of the wild-type CCC2 gene and the D627A, S258A, S258D, S971A, and S258A/S971A mutant genes were as described previously (10).

Protein Expression and Protein Determination—*Sf*9 cells were infected with recombinant baculovirus containing the wild-type, D627A, S258A, S258D, S971A, and S258A/S971A Ccc2 genes (21). As a control, infections were routinely performed with the empty plasmid vector (MOCK). The variants constructed are represented graphically in Fig. 1*A*, and the proposed catalytic cycle is represented in Fig. 1*B* (10). Protein expression was measured using immunodetection with anti-Ccc2 antibody (10) and an ECL™ chemiluminescence kit (GE Healthcare). Total protein content was determined using the micro BCA™ protein assay (Pierce), and proteins were

separated on 10% SDS-PAGE (22). Protein loading on gels was evaluated by Coomassie Blue or silver staining, as indicated.

Regulatory Phosphorylation—100 μg of S*f*9 membrane fractions containing either Ccc2 wt or the variants S258A, D627A, S258D, S971A, or S258A/S971A were suspended in a phosphorylation buffer containing 10 mM $MgSO_4$, 20 mM MOPS-KOH (pH 7.4), 1 mM DTT, and additives as indicated in the legend to Fig. 4, to a final volume of 100 μl. Reactions were started with [γ-^{32}P]ATP (100 μM, 2 μCi/nmol) and stopped after 30 min at 30 °C with 10 μl of CHAPS 1% (w/v). Samples were left at room temperature for 30 min before the volume was adjusted to 1 ml with ice-cold water, followed by 10 μl of a mixture of protein A-agarose and the Ccc2-specific antibody (1:1). Samples were left overnight at 4 °C with gentle stirring. Immunoprecipitation was carried out as described previously (17). The resulting immunoprecipitated protein was suspended in Laemmli electrophoresis sample buffer and applied to 7% alkaline gels. The gels were exposed to PhosphorScreen for 24 h and analyzed on a Phosphoimager using OptiQuant™ software (PerkinElmer). Endogenous PKA activity in S*f*9 membranes was assayed as in (23) with the exception that histone 2B was used in place of histone 8.

Catalytic Phosphorylation (Aspartylphosphate Formation)—Catalytic phosphorylation was measured as previously described (10). Briefly, 50 μg of S*f*9 membrane fractions containing Ccc2 wt, S258A, S258D, S971A, S258A/S971A, or D627A were incubated in a phosphorylation buffer containing 20 mM Bis-Tris propane (pH 5.8), 200 mM KCl, and 5 mM $MgCl_2$ in the presence or absence of $PKAi_{5-24}$. The mixtures were preincubated on ice (~4 °C) for 30 min prior to addition of [γ-^{32}P]ATP (5 μM, 10 μCi/nmol). Reactions were stopped with 40% (w/v) TCA after the time intervals shown in each figure and centrifuged at 18,000 × *g* for 10 min; the pellets were washed three times with ice-cold water, solubilized, and resolved on acidic gels (24). Densitometry of the ^{32}P-signal was carried out after exposure of the gels, as described above.

Phosphorylation Data Normalization—To compare the phosphorylation data obtained from different gels, we defined a "reference experiment" that was performed each time a new gel was run. Namely, in each gel one lane was dedicated to the wild-type phosphoenzyme measured after reacting with [γ-^{32}P]ATP for 1 min. Once the ^{32}P levels were measured on the gel, they were corrected for the background phosphosignal encountered at 110 kDa with the non-phosphorylating D627A mutant and for the amount of protein (Coomassie blue staining of the 110 kDa band). The result for the wild type at 1 min (same specific activity for [γ-^{32}P]ATP and same gel) was taken as 100%. This procedure allowed experiments to be compared, irrespective of the exposure time (see Figs. 5–11). Regulatory phosphorylation data were also normalized with the data obtained from the wild type regulatory phosphoenzyme (Fig. 4), except that in this case silver staining was used for protein detection.

Measurement of Hydroxylamine Sensitivity—In some experiments (Fig. 5), the effect of 2 M hydroxylamine on the phosphoenzyme levels was assayed. The sensitivity to hydroxylamine was investigated by catalytic phosphorylation assays of Ccc2 wt, S258A, S258D, S971A, and S258A/S971A, as previously described (25). Briefly, after precipitation with TCA the sediments of samples run in parallel were washed twice with ice-cold water and resuspended in 0.5 ml of a mixture containing 2.0 M hydroxylamine and 40 mM citrate buffer adjusted to pH 5.5 with NaOH. After sequential washing with TCA and ice-cold water, the samples were prepared for the acidic gels. The total hydroxylamine-resistant phosphorylation at 110 kDa in the four variants was subtracted from the total phosphorylation after correction for the total amount of protein evaluated by Coomassie staining as described previously (10, 24). The hydroxylamine-resistant phosphorylation levels in Ccc2 wt, S258A, S971A, S258A/S971A, and S258D averaged ~20% of the total corresponding phosphorylation.

ADP-induced Dephosphorylation Experiments—To evaluate the proportions of high- and low-energy aspartylphosphate formed upon phosphorylation of different Ccc2 variants, membranes of S*f*9 cells expressing S258D, S971A, or S258A/S971A were phosphorylated by 5 μM [γ-^{32}P]ATP for 1, 2, or 3 min as described above, and 10 μM ADP was added. The reaction was stopped 10, 20, or 30 s later. The decrease in phosphoenzyme (% of the corresponding level before ADP addition) corresponds to the copper-bound high-energy aspartylphosphate (^{Cu}E~P) that is able to react with ADP to form ATP and dephosphorylate the enzyme.

Statistics—Statistical differences were verified by 2-way ANOVA, followed by a Newman-Keuls post-test, unpaired *t* test or Mann-Whitney test as required, and the significance level was set at $p < 0.05$.

Analysis of Primary Structure and Alignments of Ccc2, ATP7A, and ATP7B—The tool NetPhosK 1.0 (26) was used to search for possible serine, threonine, and tyrosine residues that exhibit high scores for phosphorylation by different protein kinases, according to the consensus sequences. The online tool Clustalw2 was used to compare the protein primary structures of Ccc2, ATP7A, and ATP7B, and to search for the motif preferentially recognized by PKA (27) in the region near the first transmembrane domain in human Cu(I)-ATPases, as previously carried out for Lys-Lys-Asn-Ser^{258}-Ile in Ccc2 (17). The potential site for PKA in this region was predicted using the pkaPS tool (28).

RESULTS

Relevance of PKA-phosphorylatable Ser^{258} *in Vivo: Effect on Copper Homeostasis*—The experiments depicted in Fig. 2 demonstrate that in addition to its influence on the catalytic cycle "*in vitro*" (17), the presence of the serine residue with the highest score for PKA in Ccc2 (Ser^{258}) is important for copper transport. When yeast cells were challenged to grow in media containing very low copper and extremely limited iron (1 mM ferrozine), the S258A mutant grew more slowly, and this became significant after 20 h (Fig. 2, *left*). When the medium was supplemented with high (500 μM) copper, *i.e.* when the yeast cells could process the metal they need without participation of Ccc2, all variants including the non-func-

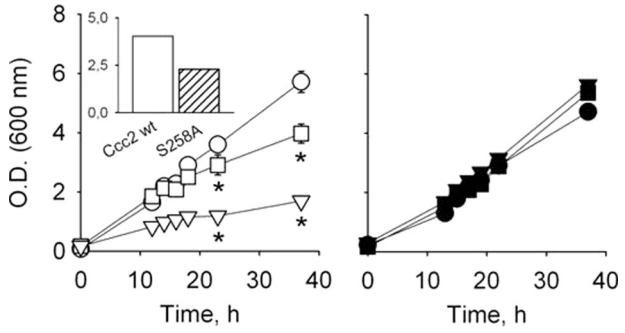

FIGURE 2. **Importance of Ser^{258} for copper homeostasis *in vivo*.** Growth curves of yeast expressing Ccc2 wt (*circles*), S258A (*squares*), and D627A (*triangles*) at 30 °C in two different media. *Left*, growth curves in iron and copper-limited medium (*open symbols*). The *inset* represents A_{600} at 38 h for Ccc2 wt and S258A yeast cell cultures (as indicated) after correction for the non-functional D627A mutant. *Right*, yeast growth in copper-supplemented medium (*closed symbols*). Composition of the media is described under "Experimental Procedures." Data are mean ± S.E. of three separate experiments.

tional D627A mutant of Ccc2 grew at the same rate and reached the same level after 38 h (Fig. 2, *right*). Previous studies have demonstrated that this variant, where the Asp^{627} was replaced with Ala, does not complement in plate assays (10). The effect of the presence or absence of Ser^{258} on cell yeast homeostasis is better appreciated when the growing rate of Ccc2 wt and S258A are corrected for that of D627A (*inset* in Fig. 2, *left*).

Measurement of PKA Activity in Sf9 Membranes—Given the physiological relevance of Ser^{258} for yeast cell homeostasis and its possibly central role in concerted regulatory PKA-mediated phosphorylations involving other residues, the following control experiments were designed to investigate whether S*f*9 cells expressing different Ccc2 variants contain significant amounts of PKA in their membranes. Fig. 3*A* demonstrates that S*f*9 membrane fractions house membrane-bound PKA that can interact with and catalyze phosphorylation of the different Ccc2 variants expressed via baculovirus. Four types of membrane preparation were assayed for PKA immunoreactivity employing a specific antibody against the α-catalytic subunit of the kinase. Membrane fractions expressing different variants (Ccc2 wt, D627A, and S258A) and MOCK (membranes from cells transfected with wild-type baculovirus) demonstrated equivalent expression of the PKA α-catalytic subunits, which co-migrated with the purified protein used as a control. To verify that the membrane-bound kinase was catalytically active, two S*f*9 membrane preparations (Ccc2 wt or MOCK) were incubated under phosphorylating conditions in the presence of an excess of histone 2B (1.5 mg/ml), a well-known substrate for different protein kinases including PKA (27) (Fig. 3*B*). Histone 2B phosphorylation decreased by ~50% when the specific PKA inhibitor, the peptide 5–24 ($PKAi_{5-24}$; 100 nM), was added to the reaction medium. Therefore, PKA is responsible for half the kinase activity in S*f*9 membrane fractions and endogenous membrane-associated PKA is suitable for studying the regulatory phosphorylation of the heterologously expressed copper pump variants.

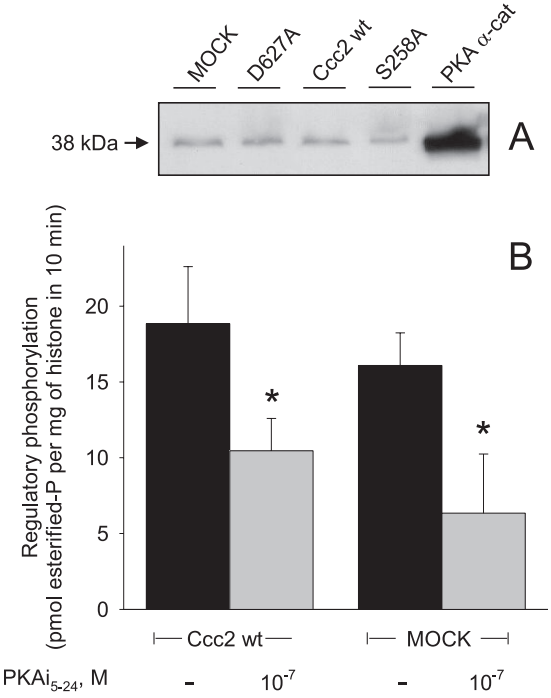

FIGURE 3. **Protein kinase A activity in S*f*9 membranes allows regulatory phosphorylation in Ccc2 and its mutants to be detected.** *A*, membranes from S*f*9 cells expressing D627A, Ccc2 wt, S258A, or transfected with an empty bacmid (MOCK) were electrophoretically separated and subsequently immunodetected with the PKA-specific polyclonal antibody, as described under "Experimental Procedures." The extreme *right lane* was loaded with five units of purified PKA α-catalytic subunit as a positive control. *B*, densitometric representation of the phosphorylation of histone 2B (1.5 mg/ml) by membrane-anchored protein kinases of S*f*9 cells and sensitivity to the inhibitor $PKAi_{5-24}$. Bars represent mean ± S.E. of >3 determinations. Phosphorylation was carried out as described under "Experimental Procedures," with the use of membranes expressing Ccc2 wt or from S*f*9 cells transfected with empty plasmid (MOCK) in the absence or presence of 100 nM $PKAi_{5-24}$, as indicated on the abscissa. *: different from histone 2B phosphorylation with no PKA inhibitor. The data were corrected for the phosphorylation measured without histone (usually <10% of the total phosphorylation).

Mutation of Ser^{258} to Ala Leads to an Overall Decrease in Cu(I)-ATPase Regulatory Phosphorylation whereas Mutation of Ser^{971} Is Associated with a Global Increase in This Phosphorylation—To test whether the active endogenous membrane-bound PKA phosphorylated Ccc2, and whether mutation of Ser^{258} and Ser^{971} to Ala altered the regulatory phosphorylation pattern of the ATPase, membrane fractions containing either Ccc2 wt, S258A, S971A, or the double mutant S258A/S971A were subjected to a regulatory phosphorylation assay with or without 100 nM $PKAi_{5-24}$ (Fig. 4). Inhibition of endogenous PKA by $PKAi_{5-24}$ decreased total Ccc2 wt phosphorylation by ~35% and there was a comparable decrease in S258A. The remaining phosphorylation of this mutant was unaffected by $PKAi_{5-24}$, suggesting that it is mediated by kinases other than PKA. In the "phosphomimetic" S258D mutant, in which an Asp residue replaces Ser, the level of regulatory phosphorylation and the lack of response to $PKAi_{5-24}$ were comparable with S258A. In contrast, mutation of Ser^{971} led to a large global increase in regulatory phosphorylation including a parcel that is sensitive to $PKAi_{5-24}$, whether Ser^{258} is present or not. These observations indicate that Ser^{971} exerts negative control on other residues in Ccc2

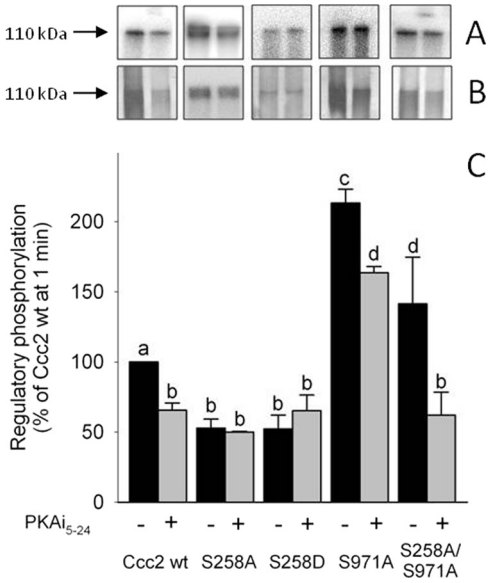

FIGURE 4. **PKA-mediated phosphorylation of Ccc2 and its variants.** *A,* autoradiograms of the 110-kDa band of representative alkaline gels after SDS-PAGE in the absence (*black bars*) or presence of 100 nM $PKAi_{5-24}$ (*gray bars*) (represented in *C*) on the regulatory phosphorylation of Ccc2 wt, S258A, S258D, S971A, and S258A/S971A. Regulatory phosphorylation and resolution of the bands in alkaline gels were carried out as described under "Experimental Procedures," with a simultaneous "reference regulatory phosphorylation" of Ccc2 wt taken as 100%, using media with the same specific activity for [γ-^{32}P]ATP and resolution in the same gel. *B,* silver staining of the corresponding gels presented in *A. C,* densitometric representation of >4 experiments (mean ± S.E.). Different *lowercase letters* above the columns indicate significant differences ($p < 0.05$).

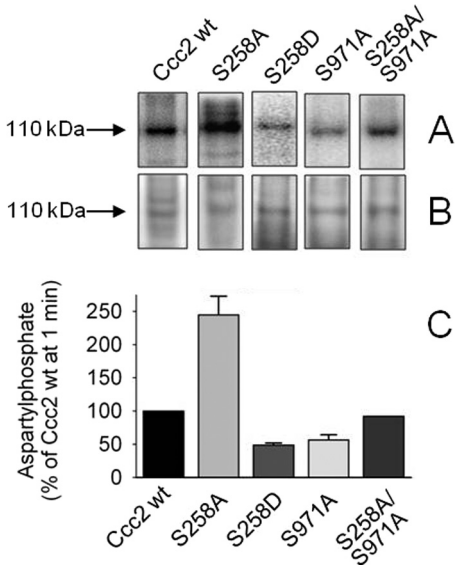

FIGURE 5. **Catalytic, hydroxylamine-sensitive phosphorylation of Ccc2 and its variants.** *A*, Sf9 membranes containing Ccc2 wt, S258A, S971A, or S258A/S971A were phosphorylated for 1 min with [γ-^{32}P]ATP as described under "Experimental Procedures," and the proteins were resolved on acidic gels, *B*, Coomassie Blue-stained gels demonstrating the 110 kDa bands used to correct the phosphorylation levels. *C*, densitometric representation (mean ± S.E. of >3 experiments) of Ccc2 wt, S258A, S258D, or S971A and two experiments using S258A/S971A that agreed within 15%. Phosphorylation of Ccc2 wt was taken as 100% (see normalization of phosphorylation data under "Experimental Procedures"). Bars represent aspartylphosphate formation corrected for the corresponding hydroxylamine-resistant phosphorylation (average ~20% of total phosphorylation).

that are targets for PKA and other kinases. Using the tool NetPhosK 1.0 (26), we encountered more than 40 phosphosites (excluding those detected in the transmembrane domains) that exhibit high scores for phosphorylation by PKA, PKC, casein kinase I, and casein kinase II, among other kinases.

Different Aspartylphosphate Levels after Single or Combined Mutations of Distinct Serines—Fig. 5 demonstrates that the absence of phosphorylatable serines with a high score for PKA recognition (17) altered the yield of aspartylphosphate, and that the amount of phosphorylated intermediate depended on the specific mutated serine. Catalytic phosphorylation at 1 min was 2.5 times higher in S258A than in Ccc2 wt, 40% lower in S971A and unchanged in the double-mutant S258A/S971A. The S258D substitution caused 50% inhibition of the catalytic phosphorylation observed at 1 min. These results demonstrate that different roles can be attributed to these regulatory sites in terms of controlling the levels of phosphorylated intermediate during the catalytic cycle of Ccc2. Therefore, the time courses of aspartylphosphate formation were investigated and compared.

Rate of Catalytic Phosphorylation with Ccc2 wt, S258A, and S258D—Replacement of Ser^{258} with Ala decreased the rate of E~P → E-P conversion (step 3 in Fig. 1*B*; see Ref. 17). The aim of the experiments presented in Fig. 6 was to examine whether the Ser^{258} → Ala mutation altered the kinetic parameters of aspartylphosphate formation during the early steps of the catalytic cycle. The kinetics of catalytic phosphorylation can be described by Equation 1,

$$EP_t = Burst + EP_{max}(1 - e^{-kt}) \quad \text{(Eq. 1)}$$

where k is the first-order rate constant of phosphorylation, and EP_t is the phosphoenzyme level after normalization. EP_t corresponds to the sum of the high- and low-energy forms (E~P + E-P). The burst corresponds to the initial and more rapid velocity of phosphorylation that reflects the ratio between the copper-bound and copper-free unphosphorylated forms of the pump (^{Cu}E:E). When Ser^{258} was mutated to Ala, the rate constant of phosphorylation decreased by ~50% and the burst dropped 8 times. Using the S258D mutant (Fig. 7), the burst was recovered but k had the lowest value among all variants here studied. In contrast to the transient catalytic phosphorylation of the wild-type Ccc2, which reaches its maximum after 1 min and slowly decreases (10), the catalytic phosphoenzyme of both mutants is still high after 10 min (300 and 125%). The kinetic parameters obtained with these mutants are summarized in Table 1.

Inhibition of PKA by $PKAi_{5-24}$ Decreases Aspartylphosphate Formation in Ccc2 wt but Not in S258A or S258D—Figs. 8 and 9 demonstrate that the formation of aspartylphosphate in the catalytic cycle of Ccc2 is directly influenced by PKA-mediated regulatory phosphorylation of Ser^{258}. Dose-dependent inhibition of aspartylphosphate formation at 1 min by the $PKAi_{5-24}$ peptide was only observed with the wild type protein. Catalytic phosphorylation of the mutant S258A was insensitive to $PKAi_{5-24}$ (compare *left* and *right panels* in Fig. 8), and so was that obtained with S258D (Fig. 9*A*). *Panel B* in Fig. 9 demonstrates that in the "phosphomimetic" mutant the ADP-sensitive fraction of aspartylphosphate gradually de-

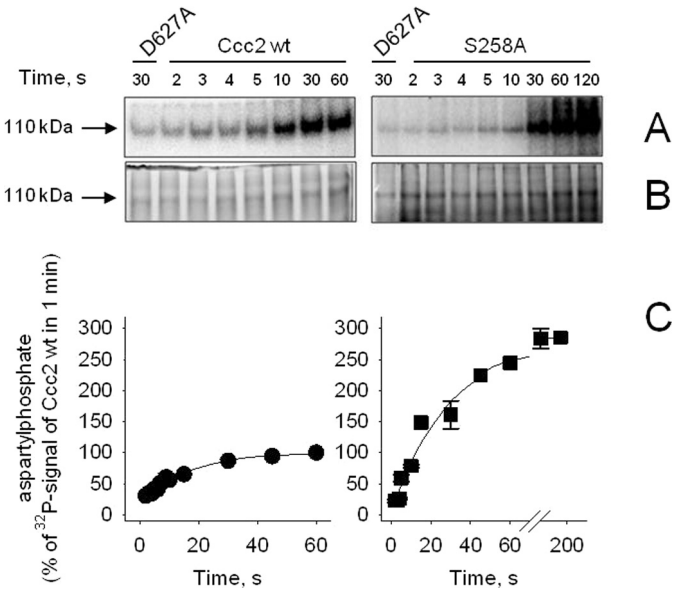

FIGURE 6. **Time course of aspartylphosphate formation of Ccc2 wt and S258A.** *A*, autoradiogram of the 110-kDa band from a representative gel after resolution of the proteins by acidic gel electrophoresis. Membranes of S*f*9 cells expressing Ccc2 or S258A were phosphorylated with [γ-^{32}P]ATP for the indicated times. *B*, Coomassie Blue staining of the same gels. *C*, densitometric representation of the time-course of phosphorylation obtained from autoradiograms corrected for the corresponding amount of protein loaded in each lane and for the background signal simultaneously measured with the non-phosphorylating D627A mutant. The phosphoenzyme levels were normalized, taking phosphorylation of Ccc2 wt at 1 min as the reference (see "Experimental Procedures"). Data are mean ± S.E. of 5–7 time course runs with different time intervals. When not shown, the S.E. was smaller than the symbol size. The *smooth lines* were adjusted to the mean experimental points with the use of Equation 1 (see text), using the mean values (Table 1) of the rate constants of phosphorylation, burst, and EP_{max} calculated for each individual experiment.

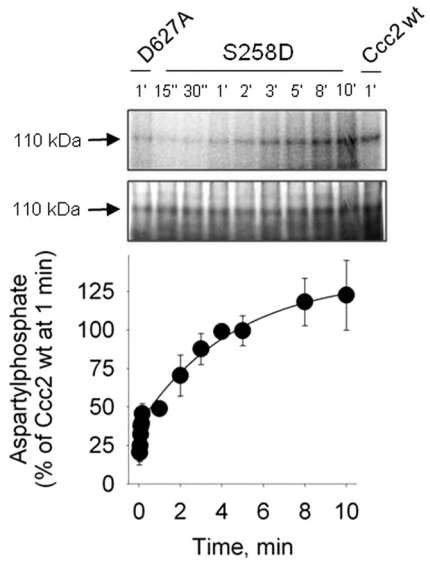

FIGURE 7. **Time course of aspartylphosphate formation of the "phosphomimetic" mutant S258D.** *Top*, autoradiogram of the 110-kDa band from a representative gel (at the indicated phosphorylation times) after resolution of the proteins by acidic gel electrophoresis. Membranes of S*f*9 cells expressing S258D were phosphorylated with [γ-^{32}P]ATP for the times indicated on the abscissa. *Middle*, Coomassie Blue staining of the same gels. *Bottom*, densitometric representation of the time course of phosphorylation obtained from autoradiograms corrected for the corresponding amount of protein loaded in each lane and for the background signal simultaneously measured with the non-phosphorylating D627A mutant. The phosphoenzyme levels were corrected for protein loading and background phosphosignal. For normalization, phosphorylation of Ccc2 wt at 1 min was taken as the reference (see "Experimental Procedures"). The smooth line was adjusted to the experimental points by fitting Equation 1 to the experimental values. Data are mean ± S.E. of four time course runs.

creased as long as phosphorylation progressed (compare with Fig. 4 in Ref. 17.

The observations that Ser^{258} is required for phosphorylation of other PKA-phosphorylatable residues (Fig. 4), that the pattern of Ccc2 regulatory phosphorylation changes when Ser^{971} is mutated to Ala (Fig. 4), and that S258A is insensitive to $PKAi_{5-24}$ (Fig. 8), led us to investigate a possible modulatory role for Ser^{971}.

Ser^{971} *Is Required to Accelerate Early Steps of Phosphorylation and Allows the Breakdown of the Low Energy Aspartylphosphate E-P*—To investigate whether Ser^{971} plays a role in the catalytic cycle, the time course of aspartylphosphate formation in S971A was investigated. Fig. 10*A* demonstrates that up to 1 min, aspartylphosphate levels in the mutant S971A increased very slowly ($k = 0.007\ s^{-1}$; Table 1). The recovery of the burst (Table 1) is probably due to preservation of Ser^{258} in the S971A mutant. At longer time intervals the phosphoenzyme levels continued to increase, surpassing those obtained with Ccc2 wt, providing evidence that dephosphorylation was impaired by the mutation of Ser^{971}. Interestingly, and in contrast to S258A (17), the phosphorylated intermediate accumulated predominantly in the low-energy E-P form; the parcel of ADP-sensitive aspartylphosphate remained nearly constant as long as the total amount of phosphoenzyme increased (Fig. 10*B*, *arrows*). These alterations in catalysis could be ascribed to the release of other regulatory (inhibitory) sites that appear to be controlled by Ser^{971} (Fig. 4). Fig. 10*C* demonstrates that catalytic phosphorylation of S971A became irresponsive to the PKA inhibitor.

TABLE 1

Kinetic parameters for the catalytic phosphorylation of Ccc2 wt, S258A, S258D, and S971A

The kinetic parameters (EP_{max} and rate constant) were determined by fitting Eq. 1 (see text) to the experimental points and $t_{½}$ was calculated by ln 2/*k*. Experimental values were normalized using EP_{max} of Ccc2 wt as a reference (100%); see phosphorylation data normalization under "Experimental Procedures."

	EP_{max}	Rate constant (*k*)	$t_{½}$	Phosphorylation burst
		s^{-1}	*s*	
Ccc2 wt	100	0.057 ± 0.007	13.5 ± 1.6	19.1 ± 3.2
S258A	284.2 ± 2.7	0.030 ± 0.004[a]	23.7 ± 1.7	2.4 ± 1.1[b]
S258D[c]	96.2 ± 7.7	0.0036 ± 0.0008	192.5 ± 42.4	38.4 ± 4.6
S971A[d]	231.4	0.007	99.0	11.1

[a] $p < 0.05$ (unpaired *t* test).
[b] $p < 0.01$ with respect to Ccc2 wt (Mann-Whitney rank sum test) ($n \geq 4$ time course runs covering various time intervals). Experimental values were normalized using EP_t of Ccc2 wt as a reference (100%).
[c] $n \geq 4$ time course runs covering various time intervals.
[d] Kinetic parameters were obtained by fitting values ($n = 2$ time course runs) that agreed within 15% or less.

Double Mutation in Ser^{258} *and Ser*^{971} *Reveals a Sequential Role for These Residues during Catalysis*—At a reaction time of 1 min, the double-mutant S258A/S971A displayed comparable levels of aspartylphosphate to the Ccc2 wt (Fig. 11, *A* and *B*), which could be ascribed to the combination of different rates of phosphorylation and dephosphorylation that are influenced by Ser^{258} and Ser^{971}. However, the most striking

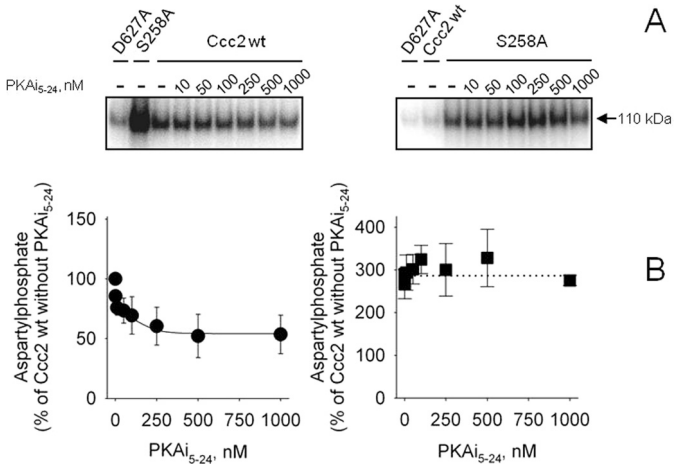

FIGURE 8. **PKA inhibition decreases aspartylphosphate formation at the catalytic cycle in Ccc2 wt but not in S258A.** *A*, autoradiogram of the 110 kDa band from a representative gel after resolution of the proteins by acidic gel electrophoresis. Membranes of *Sf*9 cells expressing Ccc2 wt or S258A were phosphorylated for 1 min with [γ-^{32}P]ATP and increasing concentrations of $PKAi_{5-24}$, as indicated on the abscissa. *B*, densitometric representation of the autoradiograms demonstrating the levels of aspartylphosphate after 1 min in the presence of the $PKAi_{5-24}$ concentrations given on the abscissa. Data are mean ± S.E. of >3 determinations. The data obtained from autoradiograms were corrected for the corresponding amount of protein loaded on each lane and for the background signal simultaneously measured with the non-phosphorylating D627A mutant (as shown on the top of the autoradiogram). For the inhibition of Ccc2 wt phosphorylation by $PKAi_{5-24}$ the smooth line was adjusted to the experimental points, using the general equation of inhibition $EP_i = EP_o \times [I]/([I] + I_{0.5}) + EP_r$, where EP_i is the aspartylphosphate level at each $PKAi_{5-24}$ concentration, EP_o is the aspartylphosphate level in the absence of inhibitor, [I] is the concentration of $PKAi_{5-24}$, $I_{0.5}$ is the $PKAi_{5-24}$ required for half-inhibition of the catalytic phosphorylation (50 nM) and EP_r corresponds to the catalytic phosphorylation that is insensitive to PKA inhibition. The phosphoenzyme level of Ccc2 wt in the absence of PKA inhibitor was taken as the reference (100%).

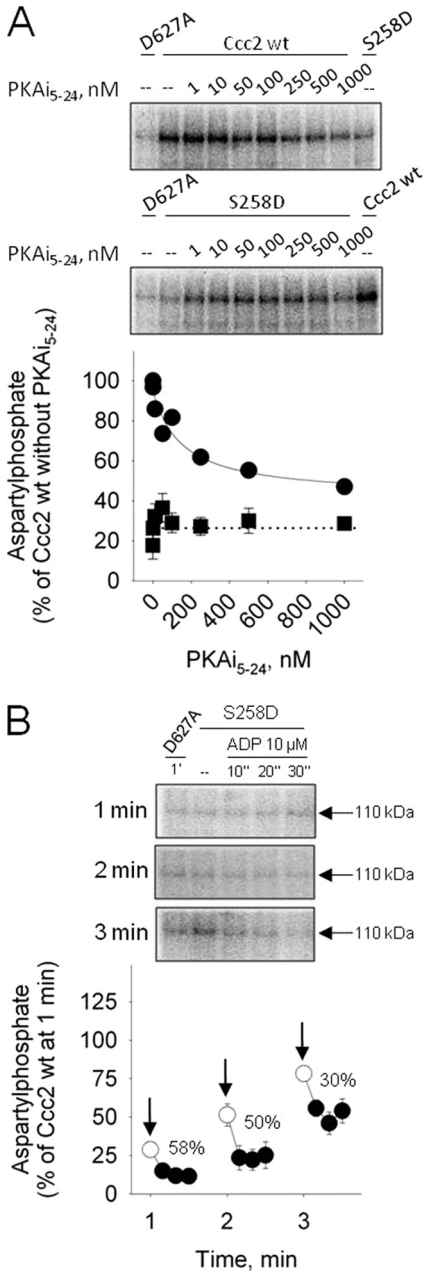

FIGURE 9. **Influence of $PKAi_{5-24}$ and ADP on the aspartylphosphate levels obtained with the phosphomimetic S258D mutant.** *A*, *upper* and *lower* autoradiograms correspond to representative experiments demonstrating aspartylphosphate levels of Ccc2 wt and S258D at 1 min respectively, in the presence of various concentrations of $PKAi_{5-24}$. The panel demonstrates the densitometric representation of the autoradiograms obtained with Ccc2 wt (*circles*; $n = 2$) and S258D (*squares*; mean ± S.E., $n = 4$). Data were normalized and aspartylphosphate levels of Ccc2 wt at 1 min without inhibitor were regarded as 100%. The function described in the legend of Fig. 8 was adjusted to the Ccc2 wt data by non-linear regression. *B*, representative autoradiograms obtained with membranes of *Sf*9 cells expressing S258D that were phosphorylated by [γ-^{32}P]ATP for 1, 2, or 3 min (*arrows*) and supplied with ADP for 10, 20, or 30 s. The figure demonstrates the densitometric representation of three assays (mean ± S.E.). The decrease in phosphoenzyme (% of the corresponding level before ADP addition) corresponds to the ADP-sensitive $^{Cu}E\sim P$.

difference between the two serines was that mutation of Ser^{258} impaired conversion of the high-energy aspartylphosphate (17) whereas mutation of Ser^{971} inhibited the breakdown of the low-energy intermediate. Sensitivity to ADP was restored in the double-mutant (Fig. 11, *A* and *B*) and, as in the case of S258A and S971A, sensitivity toward $PKAi_{5-24}$ disappeared (Fig. 11*C*).

Prediction of PKA Phosphorylation Sites: Identification of Topologically Related Sites in Ccc2, ATP7A and ATP7B—Alignment of Ccc2 with human Cu(I)-ATPases revealed strong homology in the region surrounding the predicted PKA phosphorylation consensus sequence, close to the first transmembrane domain (Fig. 12). ATP7A and ATP7B share the key residues with Ccc2 around Ser^{653} that are necessary for PKA recognition and phosphorylation: two basic clustered residues before and one hydrophobic residue after the corresponding phosphorylatable serine (27–29).

DISCUSSION

Having previously demonstrated that Ccc2, the yeast homologue of mammalian Cu(I)-ATPases, is phosphorylated by kinases, and that PKA, acting on a serine residue (Ser^{258}) with the highest predicted score for phosphorylation, is a pivotal modulator of the key step during catalysis (energy interconversion and copper translocation (17)), we now demonstrate that: (i) Ser^{258} is essential for *in vivo* copper homeostasis when copper and iron in the medium are limiting; (ii) Ser^{258} and Ser^{971} influence other regulatory sites; (iii) there is interplay between Ser^{258} and Ser^{971}; (iv) these regulatory sites play specific roles in distinct and key

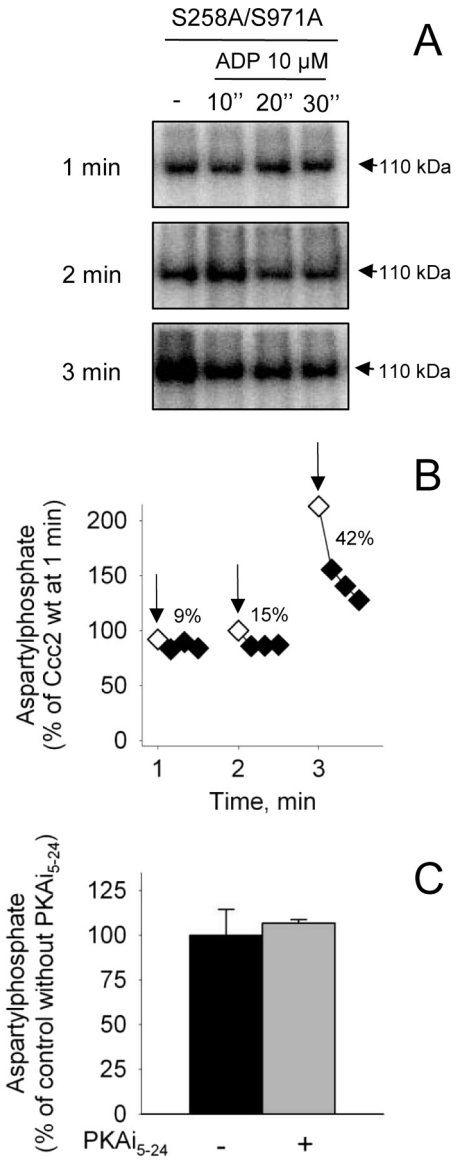

FIGURE 10. **S971A aspartylphosphate: time course of formation, ADP sensitivity, and influence of PKAi$_{5-24}$.** *A*, membranes of S*f*9 cells expressing S971A were phosphorylated with [γ-^{32}P]ATP at the indicated times. The autoradiogram depicts a representative experiment on the short time range scale (see *inset*). The autoradiograms in *B* with no ADP at 1, 2, and 3 min are representative of long time range phosphorylations. The figure presents the densitometric representation of six time course runs covering various time intervals (mean ± S.E.). The *smooth curve* was adjusted to the points by Equation 1 (see text). The *inset* depicts phosphorylation at shorter times for better visualization. The phosphoenzyme levels were normalized, taking phosphorylation of Ccc2 wt at 1 min as a reference (100%). *B*, representative autoradiograms obtained with membranes of S*f*9 cells expressing. S971A that were phosphorylated by [γ-^{32}P]ATP for 1, 2, or 3 min (*arrows*) and supplied with ADP for 10, 20 or 30 s. The figure presents the densitometric representation of three assays (mean ± S.E.). The decrease in phosphoenzyme (% of the corresponding level before ADP addition) corresponds to the ADP-sensitive ^{Cu}E~P. *C*, aspartylphosphate levels of S971A were measured at 1 min in the absence or presence of 1000 nM PKAi$_{5-24}$.

steps during the catalytic cycle of ATP hydrolysis and active copper transport mediated by Ccc2. Therefore, the long-range intramolecular communications between these two serines ensure an appropriate sequence of events through the catalytic cycle.

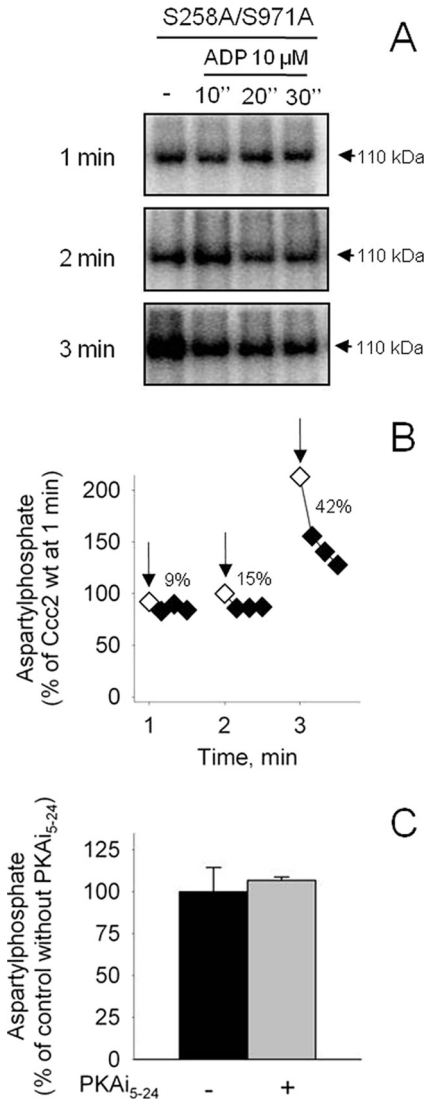

FIGURE 11. **ADP and PKAi$_{5-24}$ sensitivity of S258A/S971A aspartylphosphate.** *A* and *B*, membranes of S*f*9 cells expressing S258A/S971A were phosphorylated by [γ-^{32}P]ATP for 1, 2, or 3 min (*arrows*) and supplied with ADP for 10, 20, or 30 s. The data obtained from autoradiograms were corrected for the corresponding amount of protein loaded on each lane and for the background signal simultaneously measured with the non-phosphorylating D627A mutant (as shown at the top of the autoradiogram). *A*, representative autoradiogram; *B*, densitometric representation of two experiments that agreed within 15%. *C*, aspartylphosphate levels of S258A/S971A were measured at 1 min in the absence or presence of 1000 nM PKAi$_{5-24}$. The phosphoenzyme level of the Ccc2 wt in the absence of PKA inhibitor was taken as a reference (100%).

S*f*9 cells used to express Ccc2 and its variants have abundant and equivalent amounts of PKA associated with the cell membranes, as demonstrated by immunoanalysis in Fig. 3*A*. We exploited this fact in evaluating the PKAi$_{5-24}$-sensitive kinase activity of the membranes (Fig. 3*B*). The high endogenous kinase activity in S*f*9 membranes is partially (~50%) due to the action of PKA, because it is inhibited to the same extent by the PKAi$_{5-24}$ peptide (Fig. 3*B*). This PKA-mediated phosphorylation is responsible for 30–40% of the total kinase-mediated phosphorylation of Ccc2 (Fig. 4). Remarkably, PKA-mediated regulatory phosphorylation of the copper pump is no longer evident when Ser^{258} is replaced by Ala (Fig. 4), though there are other

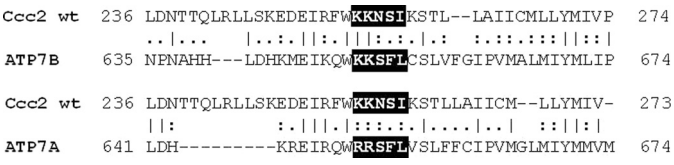

FIGURE 12. **Comparison of Ccc2, ATP7A, and ATP7B primary structures and location of a conserved PKA phosphorylation site.** Primary sequences of Ccc2 wt and human copper ATPases aligned in the neighborhood of the corresponding serine residue (Ser^{258} in Ccc2, Ser^{653} in ATP7B and ATP7A) located at the boundary between the end of the N-terminal region and the first transmembrane segment (see Fig. 1). Alignment was generated as described under "Experimental Procedures." The potential sites for PKA were predicted using the pkaPS tool (25).

serine residues with high scores for PKA-mediated phosphorylation (*e.g.* Ser^{971}) in the primary structure of Ccc2 (17). It is noteworthy that Ser^{971} exerts negative control on other residues in Ccc2 that are targets for PKA and other kinases (Fig. 4). For example, phosphosites targeted by casein kinases have been proposed in ATP7B (12) and several of them can be detected in the primary structure of Ccc2 with the use of NetPhosK 1.0. Furthermore, we can predict a threonine residue in Ccc2 (Thr^{894}) located in the large cytosolic loop after the nucleotide binding site that is highly scored for PKC phosphorylation (0.95). Several of these uncharacterized phosphosites could be copper-sensitive, as is the case in human Cu(I)-ATPases (14–16). If so, this would be physiologically important in regulating copper pumping activity under the control of Ser^{258} and Ser^{971}.

If there are other PKA-phosphosites in Ccc2 besides Ser^{258}, then why are these sites unphosphorylated when Ser^{258} phosphorylation is prevented by substitution with Ala? The fact that mutation of Ser^{258} to Ala strongly diminishes (by 50%) the overall regulatory phosphosignal, abolishes the PKAi$_{5-24}$ effect (Fig. 4) and prevents the regulatory hyperphosphorylation seen after addition of purified PKA α-catalytic subunit (17), suggests that Ser^{258} is a coordinating switch for phosphorylation of other residues. The assumption is therefore that Ser^{258} phosphorylation enables access to other phosphosites. Analogous to the regulatory phosphorylation of Ccc2 described here, a controller regulatory phosphosite has been implicated in the concerted regulation by kinases of two very different processes of electrophysiological and metabolic significance. Gating of neuronal Na^+-channels in response to membrane depolarization (30) and perilipin facilitation of lipolitic cleavage of fat droplets (31) are examples demonstrating that obligatory phosphorylation of a key residue allows convergent and synergistic kinase-mediated processes to occur.

Possibly because of its central role as a controller of a complex kinase-mediated network in Ccc2, Ser^{258} has a pronounced effect on the catalytic cycle that extends beyond that previously described for the E∼P → E-P transition (17). The fact that inhibition of aspartylphosphate formation by PKAi$_{5-24}$ occurs with the wild type Ccc2 (Fig. 7, *left panels*) whereas the response to PKAi$_{5-24}$ is completely lost in S258A (Fig. 7, *right panels*), indicates that Ser^{258} simultaneously controls kinase-mediated phosphorylating cascades acting on Ccc2 (Fig. 4) and the phosphoryl transfer from ATP to Asp^{627} at the catalytic site (Fig. 7, *step 2* in the scheme depicted in Fig. 1*B*), together with the previously described conversion of the high- to the low-energy aspartylphosphate intermediate (17). The higher level of aspartylphosphate in this mutant at 1 min (Fig. 5), and the lower rate constant of aspartylphosphate formation (Table 1) are indicative that Ser^{258} phosphorylation modulates the rate of phosphoryl transfer from ATP to Asp^{627} (*step 2* in Fig. 1*B*), supporting the idea that it could influence the coupling between ATP utilization and copper transport. In addition, the 8-fold decrease in the size of the phosphorylation burst evident with S258A (Table 1) indicates that, besides its previously demonstrated influence on the ^{Cu}E∼P → E-P + Cu_{lum} transition (17) and on the rate of aspartylphosphate formation (Fig. 6), a serine residue that can undergo PKA-mediated phosphorylation with a high score also influences the Cu + E → ^{Cu}E transition at the beginning of the cycle. The insensitivity to PKAi$_{5-24}$ of the S258A mutant (Fig. 8) does not appear to be related to abrogated PKA-mediated phosphorylation at Ser^{258} (Fig. 4) since the S258A mutation resulted in a 2.5-fold increase in aspartylphosphate levels at 1 min (Figs. 5 and 8) rather than an inhibition. On the contrary, catalytic phosphorylation of the S971A mutant at 1 min was similar to that of Ccc2 in the presence of PKAi$_{5-24}$ (Fig. 10*C*), suggesting that PKA-mediated phosphorylation at Ser^{971} also regulates Ccc2 wt turnover.

Catalytic phosphorylation of S971A is insensitive to PKAi$_{5-24}$, as in the case with S258A (Figs. 8 and 10*C*). Therefore, Ser^{971} and Ser^{258} appear to be under long range intramolecular and reciprocal control. Thus, the aforementioned results support the idea that a PKA-mediated regulatory network exerts delicate control over phosphoryl transfer to Asp^{627} at the catalytic site. Ser^{258} and Ser^{971} appear to have concerted but selective roles in the evolution of the phosphorylated intermediate during catalysis. Whereas regulatory phosphorylation of Ser^{258} is required for the ^{Cu}E∼P → E-P + Cu conversion (and copper dissociation) (17), phosphorylation of Ser^{971} is critical for the breakdown of the ADP-insensitive, low-energy phosphorylated intermediate (Fig. 10*B*), as well as influencing the beginning of the cycle (Fig. 10*A*). It is likely that Ser^{971} exerts its influence, at least in part, by acting as a switch that controls kinase-mediated phosphorylation of other residues, as revealed by the observations depicted in Fig. 4 concerning S971A and S258A/S971A.

The mutant S258D sheds some light on the mechanism by which Ser^{258} participates in the regulation of the Ccc2 catalytic cycle (Fig. 7, Table 1). Introduction of a permanent negative charge in this position increased the phosphorylation burst, which was followed by an extremely slow phosphorylation. They probably represent a rapid formation of ^{Cu}E∼P from initially available ^{Cu}E and a slower one after the E + Cu → ^{Cu}E transition (Fig. 1*B*). The increased burst and the very slow phosphoryl transfer with accumulation of E-P, together with the lower *k* measured with the S258A mutant, support the view that the presence of a stable "phosphomimetic" atmosphere in this region: (i) accelerates phosphoryl transfer, (ii) decreases the E + Cu → ^{Cu}E conversion,

and (iii) impairs hydrolysis of the phosphorylated intermediate during turnover (Fig. 1*B*). Because regulatory phosphorylation decreased in S258A, these combined results are compatible with a combination of electrostatic and non-electrostatic influences of Ser^{258} as demonstrated in other processes where phosphorylatable serines are involved (31, 32). Furthermore, they support the view of alternating regulatory phosphorylation/dephosphorylation events catalyzed by kinases and phosphatases, as early suggested for ATP7B (33).

To investigate whether there is a true sequential influence of both serines on the catalytic cycle and if Ser^{258} behaves as a switch that dictates the proper order of events during catalysis (*i.e.* the sequential formation of high- and low-energy phosphorylated intermediate) the double mutant S258A/S971A was created to examine whether a progressive increase in ADP-sensitivity can be recovered. Fig. 11 demonstrates this to be the case: a gradual accumulation of the ADP-sensitive aspartylphosphate revealed that the profile governed by the absence of Ser^{258} was encountered again, *i.e.* E∼P → E-P was impaired. The percent levels of ADP-sensitive aspartylphosphate, although they increase with time, are not as great as those found with the S258A mutant. This is certainly because the mutation of Ser^{971} in the double mutant also impairs the breakdown of the ADP-insensitive intermediate.

Apart from the well-known role of copper pumps in regulating the subcellular location and trafficking of copper (12–14), our previous work (17) in conjunction with the present study points to the significance of kinase-mediated phosphorylation during the most important steps of the Ccc2 catalytic cycle and the central role of Ser^{258} in this process. It is possible that the conserved serine in a topologically equivalent region of the polypeptide chain, *i.e.* in the short sequence of the N-terminal domain close to the first transmembrane domain, plays a similar pivotal regulatory role in other copper ATPases such as human ATP7A and ATP7B. The recently-developed prediction tool pkaPS (28) demonstrates that, as with Ser^{258} in Ccc2, a phosphorylatable Ser^{653} in human ATP7A and ATP7B is located in a conserved motif at the hinge region connecting the N-terminal domain to the core of the copper pump (Fig. 12). Therefore, this conserved serine may have an important role in PKA-mediated regulation of the human Cu(I)-ATPases, as the alignment demonstrates that Ser^{653} lies in a PKA recognition consensus sequence (27).

Ser^{653} exhibited a relatively low profile as a target for PKA in ATP7B using pkaPS and its phosphorylation was not detected by mass spectrometry (16), but its physiological relevance is unambiguous as mutating it to Tyr leads to one of the most severe and early clinical alterations in copper metabolism (34). It is interesting that a phosphorylatable serine residue at the entrance to the first transmembrane domain has also been found in the α-catalytic subunit of the ($Na^+ + K^+$) ATPase (35), and furthermore its accessibility to the kinase increases in the ^{Na}E rather than in the ^{K}E form. By analogy, the presence of copper, and therefore of ^{Cu}E, may favor the exposure of Ser^{258}, thus explaining the copper dependence of PKA-mediated phosphorylation of Ccc2.

Acknowledgments—We thank Andreia Abrantes and Gloria Costa Sarmento for helpful technical assistance.

REFERENCES

1. Lutsenko, S., Barnes, N. L., Bartee, M. Y., and Dmitriev, O. Y. (2007) *Physiol. Rev.* **87,** 1011–1046
2. Rensing, C., Fan, B., Sharma, R., Mitra, B., and Rosen, B. P. (2000) *Proc. Natl. Acad. Sci. U.S.A.* **97,** 652–656
3. Rosen, B. P. (2002) *Comp. Biochem. Physiol. A Mol. Integr. Physiol.* **133,** 689–693
4. Kaplan, J. H., and Lutsenko, S. (2009) *J. Biol. Chem.* **284,** 25461–25465
5. Bull, P. C., Thomas, G. R., Rommens, J. M., Forbes, J. R., and Cox, D. W. (1993) *Nat. Genet.* **5,** 327–337
6. Fu, D., Beeler, T. J., and Dunn, T. M. (1995) *Yeast* **11,** 283–292
7. Yuan, D. S., Stearman, R., Dancis, A., Dunn, T., Beeler, T., and Klausner, R. D. (1995) *Proc. Natl. Acad. Sci. U.S.A.* **92,** 2632–2636
8. Terada, K., Nakako, T., Yang, X. L., Iida, M., Aiba, N., Minamiya, Y., Nakai, M., Sakaki, T., Miura, N., and Sugiyama, T. (1998) *J. Biol. Chem.* **273,** 1815–1820
9. Lutsenko, S., Efremov, R. G., Tsivkovskii, R., and Walker, J. M. (2002) *J. Bioenerg. Biomembr.* **34,** 351–362
10. Lowe, J., Vieyra, A., Catty, P., Guillain, F., Mintz, E., and Cuillel, M. (2004) *J. Biol. Chem.* **279,** 25986–25994
11. Pedersen, P. L. (2007) *J. Bioenerg. Biomembr.* **39,** 349–355
12. Vanderwerf, S. M., Cooper, M. J., Stetsenko, I. V., and Lutsenko, S. (2001) *J. Biol. Chem.* **276,** 36289–36294
13. Cobbold, C., Ponnambalam, S., Francis, M. J., and Monaco, A. P. (2002) *Hum. Mol. Genet.* **11,** 2855–2866
14. Veldhuis, N. A., Valova, V. A., Gaeth, A. P., Palstra, N., Hannan, K. M., Michell, B. J., Kelly, L. E., Jennings, I., Kemp, B. E., Pearson, R. B., Robinson, P. J., and Camakaris, J. (2009) *Int. J. Biochem. Cell Biol.* **41,** 2403–2412
15. Bartee, M. Y., Ralle, M., and Lutsenko, S. (2009) *Biochemistry* **48,** 5573–5581
16. Pilankatta, R., Lewis, D., Adams, C. M., and Inesi, G. (2009) *J. Biol. Chem.* **284,** 21307–21316
17. Valverde, R. H., Morin, I., Lowe, J., Mintz, E., Cuillel, M., and Vieyra, A. (2008) *FEBS Lett.* **582,** 891–895
18. Morin, I., Gudin, S., Mintz, E., and Cuillel, M. (2009) *FEBS J.* **276,** 4483–4495
19. Maia, J. C. C., Gomes, S. L., and Juliani, M. H. (1983) in *Genes of Parasites: A Laboratory Manual* (Morel, C. M., ed) pp. 146–167, Editora Fundação Oswaldo Cruz, Rio de Janeiro, Brazil
20. Forbes, J. R., and Cox, D. W. (1998) *Am. J. Hum. Genet.* **63,** 1663–1674
21. Miras, R., Cuillel, M. Catty, P. Guillain, F., and Mintz, E. (2001) *Protein. Expr. Purif.* **22,** 299–306
22. Laemmli, U. K. (1970) *Nature* **227,** 680–685
23. Cabral, L. M., Wengert, M., da Ressurreição, A. A., Feres-Elias, P. H., Almeida, F. G., Vieyra, A., Caruso-Neves, C., and Einicker-Lamas, M. (2007) *J. Biol. Chem.* **282,** 24599–24606
24. Tsivkovskii, R., Eisses, J. F., Kaplan, J. H., and Lutsenko, S. (2002) *J. Biol. Chem.* **277,** 976–983
25. Caruso-Neves, C., Rangel, L. B., Vives, D., Vieyra, A., Coka-Guevara, S., and Lopes, A. G. (2000) *Biochim. Biophys. Acta* **1468,** 107–114
26. Blom, N., Sicheritz-Pontén, T., Gupta, R., Gammeltoft, S., and Brunak, S. (2004) *Proteomics* **4,** 1633–1649
27. Shabb, J. B. (2001) *Chem. Rev.* **101,** 2381–2411
28. Neuberger, G., Schneider, G., and Eisenhaber, F. (2007) *Biol. Direct* **2,** 1–23
29. Rodriguez, M., Li, S. S., Harper, J. W., and Songyang, Z. (2004) *J. Biol. Chem.* **279,** 8802–8807
30. Li, M., West, J. W., Numann, R., Murphy, B. J., Scheuer, T., and Catterall, W. A. (1993) *Science* **261,** 1439–1442

31. Miyoshi, H., Perfield, J. W. 2nd, Souza, S. C., Shen, W. J., Zhang, H. H., Stancheva, Z. S., Kraemer, F. B., Obin, M. S., and Greenberg, A. S. (2007) *J. Biol. Chem.* **282,** 996–1002
32. Arokium, H., Ouerfelli, H., Velours, G., Camougrand, N., Vallette, F. M., and Manon, S. (2007) *J. Biol. Chem.* **282,** 35104–35112
33. Vanderwerf, S. M., and Lutsenko, S. (2002) *Biochem. Soc. Trans.* **30,** 739–741
34. Gromadzka, G., Schmidt, H. H., Genschel, J., Bochow, B., Rodo, M., Tarnacka, B., Litwin, T., Chabik, G., and Czlonkowska, A. (2005) *Clin. Genet.* **68,** 524–532
35. Sweadner, K. J., and Feschenko, M. S. (2001) *Am. J. Physiol. Cell. Physiol.* **280,** C1017–C1026